Effect of Changing the Size of Lipid Headgroup on Peptide Insertion into Membranes

William T. Heller, Ke He, Steve J. Ludtke, Thad A. Harroun, and Huey W. Huang

Physics Department, Rice University, Houston, Texas 77005-1892 USA

ABSTRACT   Adsorption of amphiphilic peptides to the headgroup region of a lipid bilayer is a common mode of protein-membrane interactions. Previous studies have shown that adsorption causes membrane thinning. The degree of the thinning depends on the degree of the lateral expansion caused by the peptide adsorption. If this simple molecular mechanism is correct, the degree of lateral expansion and consequently the membrane thinning should depend on the size of the headgroup relative to the cross section of the hydrocarbon chains. Previously we have established the connection between the alamethicin insertion transition and the membrane thinning effect. In this paper we use oriented circular dichroism to study the effect of varying the size of the headgroup, while maintaining a constant cross section of the lipid chains, on the insertion transition. A simple quantitative prediction agrees very well with the experiment.

INTRODUCTION

Membrane active, antibiotic peptides provide simple, well-defined systems for studying peptide-membrane interactions. In particular, alamethicin, a 20-amino acid amphiphilic helical peptide (Pandey et al., 1977), exhibits two different phases of interaction with membranes (Huang and Wu, 1991). In the low concentration phase, it adsorbs to the surface of the membrane. In the high concentration phase, the peptide inserts across the membrane, resulting in the formation of pores (He et al., 1995, 1996b). We have proposed that the driving force for this transition is the membrane thinning effect (Huang, 1995). The membrane thinning effect occurs whenever a peptide is embedded in the lipid headgroups. This is apparently a common mode of interaction for amphiphilic peptides and proteins. To further characterize the membrane thinning effect, we study the effect of varying the size of the lipid headgroup on alamethicin's insertion transition. A quantitative prediction based on the membrane thinning effect is compared with experimental results.

The prime mover of protein-membrane interactions is undoubtedly hydrophobic matching. The energy cost of hydrophobic mismatch is considerable. For example, transferring a hydrophobic protein surface from an aqueous environment to an organic solvent lowers the free energy by $\sim 4k_BT/nm^2$ (Chothia, 1974). That is why amphiphilic peptides have high affinities for lipid bilayers. One common structural motif of membrane active peptides is the α-helix, with hydrophilic residues distributed on one side along the helical axis and hydrophobic residues on the other. For such amphiphilic helical peptides, an obvious hydrophobic

matching configuration is for the helix to lie parallel to the bilayer surface, with the hydrophobic side buried in the hydrocarbon region and the hydrophilic side exposed to the polar region of the bilayer. However, this is not the only possible state satisfying hydrophobic matching. At least two nonsurface states have been observed, formed by two different amphiphilic helical peptides. Alamethicin and magainin both form pores in membranes, the former in a barrel-stave fashion and the latter in a toroidal fashion (He et al., 1995, 1996b; Ludtke et al., 1996). In each case the peptide adsorbs on the membrane surface in low concentrations, but above a critical concentration, the pore states appear. The peptides satisfy hydrophobic matching in both the surface state and the pore states. To understand why the peptides change their configurations in membranes, we need to look beyond the principle of hydrophobic matching and study other possible energetics in peptide-membrane interactions.

Alamethicin interaction with diphytanoylphosphatidyl-choline (DPhPC) bilayers has been extensively studied by this laboratory. Alamethicin adsorbs on the surface of the DPhPC membrane if the peptide concentration (expressed as the peptide-lipid molar ratio P/L) is less than 1/40. As P/L increases above this critical concentration, an increasing fraction of alamethicin inserts and forms pores in the bilayer, until $P/L \geq 1/17$, when all of the alamethicin forms pores. This range of transition, $1/40 \leq P/L \leq 1/17$, is experimentally convenient. We have been able to study both the surface adsorption phase (Wu et al., 1995) and the insertion phase (He et al., 1995, 1996b) by x-ray and neutron techniques and theoretically explain the transition (He et al., 1996a). This system is also suitable for investigating the effect of lipid variations. Lipids with the same (3,7,11,15-tetramethylhexadecanoic) chains as DPhPC but with a different headgroup, for example, phosphatidic acid (PA), phosphatidylethanolamine (PE), phosphatidylglycerol (PG), and phosphatidylserine (PS), are available. By mixing a small amount of these lipids into the pure DPhPC bilayer,

we can vary the average size, the average net charge, and other properties (e.g., the extent of hydrogen bonding) of the headgroup in a continuous manner. In this way, we introduce perturbation parameters that can be varied continuously.

Indeed, the idea of mixing lipids to vary their physical properties has been utilized by many investigators. In particular, the effect of PC/PE mixture on the bilayer-to-hexagonal phase transition has been extensively studied (Hui et al., 1981; Kirk and Gruner, 1985; Epand and Bottega, 1988), and the correlations between the membrane's propensity to form the hexagonal phase and membrane protein activities have been speculated on (Hah et al., 1993; Gruner, 1994). For example, the conductance states of the single channel induced by alamethicin were found to vary with the mixing ratio of dioleoylphosphatidylethanolamine and dioleoylphosphatidylcholine (Keller et al., 1993).

Previous investigations have shown that a major contributor to the energetics of alamethicin-membrane interactions is the free energy of membrane deformation. A Hamiltonian consisting of the hydrophobic matching energy (i.e., binding energy) and the membrane deformation energy can explain the phase transition of alamethicin insertion (He et al., 1996a). In particular, the onset of insertion can be understood as follows. If peptide monomers are embedded in the headgroup region of a lipid bilayer and the bilayer is maintained in the planar configuration, the area of the headgroup region expands. The lipid chains adjust to the lateral expansion by *trans-gauche* excitations. It is known that the chain volume is essentially conserved in order-disorder transitions (Nagle and Wilkinson, 1978). Thus the hydrocarbon region will become thinner if peptides adsorb in the headgroup region. This membrane thinning effect has been measured for alamethicin (Wu et al., 1995; He et al., 1996a) and magainin adsorption (Ludtke et al., 1995). In both cases, the thinning is proportional to the peptide concentration, as expected from the simple mechanism described above. The energy of membrane thinning is proportional to the square of the change in the thickness of the bilayer, so this energy increases quadratically with the peptide concentration. Thus, even though the surface state has a lower free energy relative to the pore state at low peptide concentrations, at high enough peptide concentrations the relative energy levels between these two states are reversed—hence the onset of insertion.

What determines the critical concentration for insertion, $(P/L)^*$? We know that $(P/L)^*$ varies a great deal with the lipid composition of the membrane (Huang and Wu, 1991; Wu et al., 1995). For example, in DPhPC $(P/L)^* \approx 1/40$, in DOPC $(P/L)^* \approx 1/200$, and in DLPC $(P/L)^* < 1/300$. However, it is not clear how to correlate these results with the properties of the lipid bilayers. Unless we vary the lipid composition continuously, it is difficult to quantify the changes in the membrane properties. The previous model calculation of the Gibbs free energy (He et al., 1996a) shows that $(P/L)^*$ involves many factors, including the elastic properties of the bilayers, the binding energy difference between the surface state and the pore state, the area

expansion of the bilayer per peptide adsorbed, and the thickness-matching condition of the bilayer to the inserted peptide. These factors are potentially the basis of lipid specificities. In this paper we will concentrate on the area expansion of the bilayer per peptide adsorbed, which is directly related to the membrane thinning effect. When a small amount of DPhPE is added to pure DPhPC, the average size of the headgroup becomes smaller, whereas the chain cross section remains the same. It is then easier to accommodate the peptide adsorption in the headgroup region. Therefore, one expects that more peptides are needed to create the same thinning effect, and the critical $(P/L)^*$ will increase in a predictable way.

MATERIALS AND METHODS

1,2-Diphytanoyl-sn-glycero-3-phosphatidylcholine (DPhPC) in $CHCl_3$ and 1,2-diphytanoyl-sn-glycero-3-phosphatidylethanolamine (DPhPE) in $CHCL_3$ were purchased from Avanti Polar Lipids (Alabaster, AL). Alamethicin was purchased from Sigma Chemical Co. (St. Louis, MO). It is a mixture of components, principally alamethicin I (85% by high-performance liquid chromatography) and alamethicin II (12%), which differ by one amino acid (Pandey et al., 1977). $CHCl_3$ with 1% ethanol was purchased from EM Science (Gibbstown, NJ) and was certified 99.99% pure by gas chromatography (GC). 2,2,2-Trifluoroethanol (TFE) was purchased from Sigma Chemical Co. and was certified >99.95% pure, also by GC. All materials were used without further purification. Small batches (~10 mg) of lipid mixtures were prepared such that the mixtures contained 2%, 5%, or 10% DPhPE (in molar ratio), with the remaining lipid consisting of DPhPC. The lipid mixtures were dissolved in $CHCl_3$ at a concentration of 10 mg/ml. Alamethicin was dissolved in $CHCl_3$ at 1.5 mg/ml.

The sample preparation was similar to the method employed previously by this group (Ludtke et al., 1995). First, a quartz slide was abrasively cleaned with 200 proof ethanol and tissue paper until there were no visible traces of contaminants on the slide. Next the slide was placed in a heated bath of sulfuric/chromic acid for ~20 min. Upon removal from the acid bath, the slide was rinsed first with distilled water until there were no visible traces of acid on the slide and then with ethanol. The rinsed slide was placed in an oven (~60°C) until it was dry. The lipid and peptide solutions were deposited on the slide in amounts intended to achieve the desired peptide-to-lipid (P/L) ratio, for a total amount of lipid of 0.25–1.0 mg. The solvent was allowed to evaporate from the slide. Then a small volume (~200 μl) of 3:1 $CHCl_3$:TFE was deposited on the face of the slide. The particular ratio of the two solvents provides the appropriate surface tension near the end of the evaporation process to ensure a well-aligned sample. The sample was rocked around in a circular fashion to ensure that most of the surface of the slide (~4 cm^2) was covered with sample. This rocking motion was continued until most of the solvent had evaporated. The remainder of the solvent was allowed to evaporate to the air. The sample was then placed in a freeze drier under vacuum (~10 μm Hg). The alignment of the sample relied on self-assembly of the lipid bilayers on the surface of the substrate. The intent of this process is to force the system to form aligned multilayers. By the clarity and visible texture of the sample, it is possible to determine its uniformity and alignment qualitatively. It is also possible to determine whether the sample is in the L_α phase by observing a thick sample through crossed polarizers (Huang and Olah, 1987). Ultimately the quality of the samples can be determined by studying the CD spectra measured for the presence of artifacts such as birefringence or attenuation (Wu et al., 1990). Results showing such artifacts were discarded. The measurement for each peptide-to-lipid ratio was repeated at least once with a different sample to ensure that the results seen were reproducible.

The temperature of the sample was controlled by a feedback loop driven by the output of a solid-state temperature probe (AD 590K) from Omega Engineering (Stamford, CT). The hydration of the sample was controlled

by allowing the sample to come to equilibrium with the air in a small, sealed chamber connected to a temperature-controlled water bath. The relative humidity of the air varies in response to the temperature of the water bath. The temperature of the water bath is controlled by the feedback loop such that the relative humidity in the chamber approaches the desired level. The humidity sensor is an EMD-2000 from Phys-Chem Scientific Corp. (New York, NY). The sensor is a solid-state device, the impedance of which varies in a nonlinear fashion with the relative humidity of the air that the sensor is exposed to, with a small temperature dependence. The probe was mounted on the same surface that the sample was mounted on to ensure that the probe and the sample were experiencing the same conditions. This system provided a stable relative humidity to within 1%. The temperature of the sample was stable to within $\pm0.1°C$. The humidity sensor has an absolute accuracy of $\pm2\%$, and the temperature has an absolute accuracy of $\pm2°C$ maximum.

Circular dichroism of the oriented sample was measured with light incident normal to the substrate surface (Wu et al., 1990). Data were collected on a Jasco J-500A spectropolarimeter. The temperature and relative humidity of the sample as well as the data collection were controlled by a PC. Each sample was put through a humidity cycle containing 15 settings, ranging from ~74% to ~96%. The temperature used for the samples was $26.8 \pm 0.5°C$. The time to measure the sample at each humidity setting was ~1 h. Four sets of five scan averages were collected for each humidity setting. The first three sets usually exhibited changes with time as the sample came to equilibrium with the new relative humidity setting. The fourth set of scans was used in the analysis of the data.

The analysis of the data was similar to that employed previously in this group (Huang and Wu, 1991). Two basis spectra were obtained, one corresponding to the helical axis parallel to the incident light and another the helical axis perpendicular to the incident light (Wu et al., 1990). The spectra collected were decomposed as a linear combination of the two basis spectra to obtain the percentage of alamethicin oriented normal to the aligned multilayers. Several different peptide-to-lipid ratios, ranging from P/L = 1/40 to 1/13, were measured for DPhPC samples containing 0%, 2%, 5%, and 10% molar fractions of DPhPE.

RESULTS

The inset graph in Fig. 1 shows a series of OCD spectra collected at various relative humidities for P/L = 1/17 in 98% PC/2% PE. Such series are collected for all of the peptide concentrations and lipid compositions presented in this paper. In general, the series reflect an increasing fraction of the peptide oriented perpendicular to the membrane as the humidity increases (Huang and Wu, 1991). Each sample composition has a well-defined pattern of hydration dependence. Although our main interests are the data near full hydration, it is useful and in fact essential to collect the hydration series. First, we demanded the reproducibility of the whole series for each sample composition. Second, because it is very difficult to achieve 100% relative humidity, it is important to examine the hydration dependence near the full hydration. Third, the P/L and humidity dependence gives rise to a phase diagram (see Fig. 2 below).

Fig. 1 shows the spectra for the peptide-to-lipid ratio P/L = 1/17 at low relative humidities and high relative humidities. Four different sets of spectra are shown for different fractions of DPhPE, ranging from 0% to 10%. In the three cases of PC/PE mixtures, the low-humidity spectra correspond to cases in which most of the alamethicin is oriented parallel to the bilayers. The low-humidity spectrum of pure PC shows a nonzero lever of insertion. At high
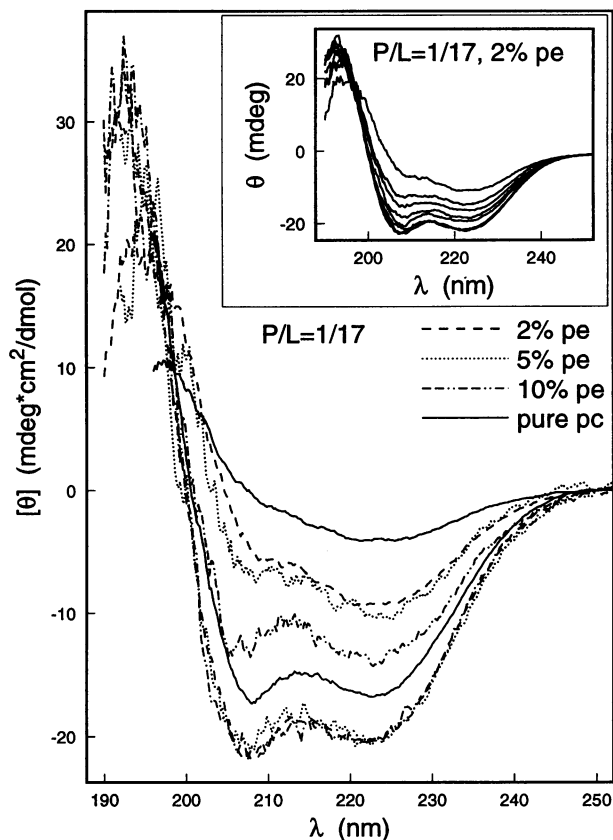

FIGURE 1 Oriented circular dichroism of alamethicin in aligned multilayers made of pure DPhPC, DPhPC/DPhPE (98:2), DPhPC/DPhPE (95:5), and DPhPC/DPhPE (9:1), all at the peptide-to-lipid molar ratio P/L = 1/17. Two spectra were shown for each sample, one in high relative humidities (~95% RH) and one in low relative humidities (~75% RH). Three low-humidity spectra in the PC/PE mixtures converge to one (at the bottom), which represents α-helices lying parallel to the plane of the bilayers. The high-humidity spectrum of alamethicin in pure DPhPC (*top spectrum*) represents α-helices oriented perpendicular to the plane of the bilayers, as analyzed by Wu et al. (1990). The low-humidity spectrum in pure DPhPC and the high-humidity spectra in PE-containing bilayers are linear combination of the parallel and perpendicular spectra. When the humidities are above 95%, the perpendicular component decreases with increasing fraction of PE. The inset shows an example (P/L = 1/17 in 2% PE) of hydration series measured for each sample.

humidities, alamethicin inserts completely into pure DPhPC bilayers. However, in PC/PE mixtures, the spectra are between the inserted spectrum and the parallel (to the bilayer) spectrum. There is a clear, consistent pattern of decreasing insertion for increasing amounts of DPhPE. (Incidentally, the entirely perpendicular spectrum in one case and the entirely parallel spectra in the three others indicate that the samples are well-aligned multilayers in all four cases.) The noise level in the spectra is typical of all of the data collected. It is due in part to the small amount of sample used, which is required to measure the samples down to as low a wavelength as possible. This noise could be averaged out, but the time required to collect the data for the entire humidity run would be greatly increased, to the point of making the experiment difficult.
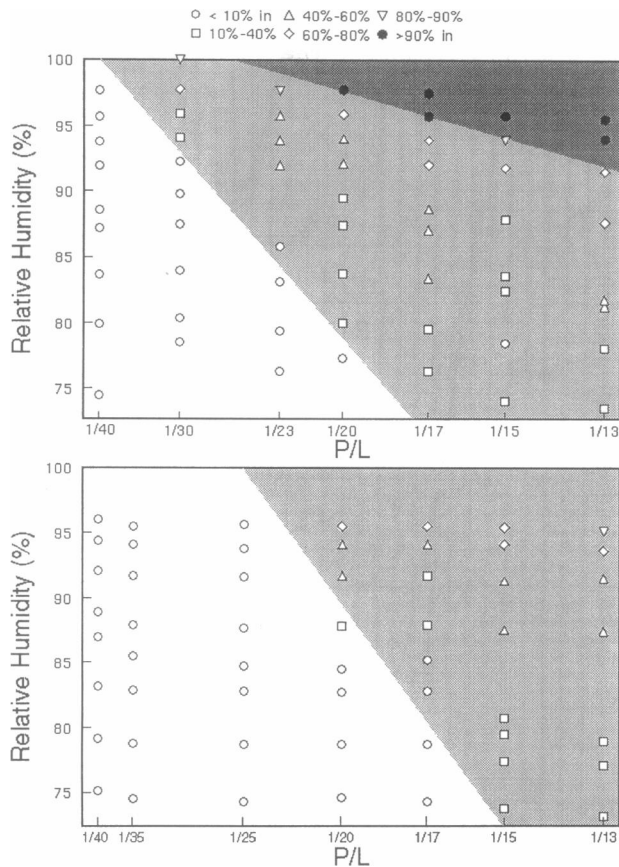
FIGURE 2   Phase diagrams of alamethicin orientation in pure DPhPC (*top*) and in DPhPC/DPhPE (9:1) (*bottom*) as functions of peptide-to-lipid molar ratio P/L and the relative humidity the samples were equilibrated with. Symbols represent various percentages of the alamethicin inserted (oriented perpendicular to the bilayer). The great majority of alamethicin is adsorbed parallel to the membrane surface in the white region. The great majority of alamethicin is inserted perpendicular in the membrane in the black region. The gray regions are coexistence regions, where a fraction of the alamethicin is inserted and the rest adsorbed on the surface.

Each CD spectrum was fit with a linear combination of two basis spectra, one for alamethicin completely inserted and one for alamethicin entirely parallel to the membrane (Wu et al., 1990). We mapped out the extent of insertion in the relative humidity-peptide concentration phase diagrams, shown in Fig. 2, for alamethicin in pure DPhPC and 90% PC/10% PE multilayers. There are clear differences between the two phase diagrams. The pure DPhPC phase diagram shows three different regions corresponding to ranges of concentration and relative humidity where the peptides are on the surface of the bilayer, inserted across the bilayer, or in a mixture of the two states, which we call the coexistence region. In contrast, the phase diagram for the 10% DPhPE system has only two of the regions, namely the coexistence region and the purely surface state region; there is no totally inserted state in the range of concentrations and hydrations shown. From the phase diagrams, we can see that there is a critical concentration for insertion (CCI), below which all peptides remain on the surface of the

bilayer for all hydrations. In the case of pure DPhPC, the CCI is roughly $(P/L)^* \approx 1/40$. In the case of 90% DPhPC/10% DPhPE, the CCI has changed to approximately $(P/L)^* \approx 1/25$. The phase diagrams also clearly indicate that the behavior of the peptide over the entire range of conditions measured has been systematically altered through the inclusion of DPhPE in the lipid bilayers. The ranges over which all levels of insertion occur have been shifted to higher concentrations.

Fig. 3 shows the maximum level of insertion (i.e., the level of insertion near the full hydration) attained for the various lipid mixtures used as a function of peptide concentration. These curves show more clearly how the inclusion of DPhPE in the bilayers affects the system near the full hydration. In the case of pure DPhPC bilayers, the maximum level of insertion levels off at total insertion near $P/L = 1/17$. In the case of PE containing systems, total insertion is not obtained at the concentrations measured. Higher peptide concentrations are not reported on in this paper, because of the difficulty of producing well-aligned samples.

DISCUSSION

The onset of insertion transition (i.e., the CCI) is defined by the equality of the peptide's chemical potentials in the surface and the insertion states: $\mu_s = \mu_I$. The chemical potential consists of two parts, the binding energy (primarily due to hydrophobic matching) $-\varepsilon$ and the energy of membrane deformation induced by the peptide f (He et al., 1996a). At the onset of insertion transition, the peptide concentration on the surface is P/L^*, whereas the concentration of inserted peptide is extremely low. f_I is the energy of membrane deformation due to an individual pore, divided by the number of monomers in a pore. On the other hand, the energy f_s is a function of P/L. Thus in the equation $\mu_s = \mu_I$, or more explicitly, $-\varepsilon_s + f_s(P/L^*) = -\varepsilon_I + f_I$, only $f_s(P/L^*)$ depends on the peptide concentration. In other
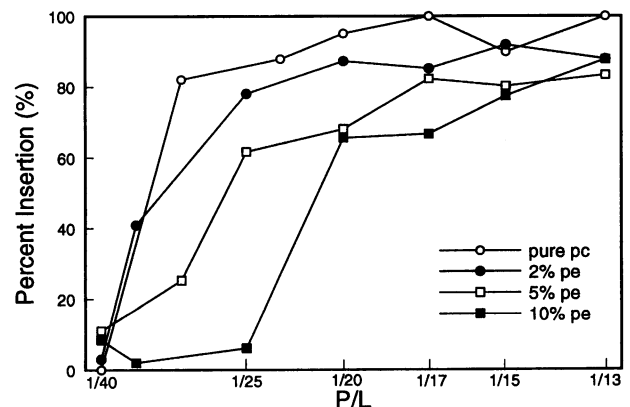

FIGURE 3   Percentage of insertion as a function of peptide-lipid ratio P/L for various DPhPE contents in DPhPC when the samples are near full hydration.

words, for a given membrane, the insertion transition occurs when the term f_s, an increasing function of P/L, reaches the value $\varepsilon_s - \varepsilon_I + f_I$. For convenience we will call this condition the critical condition.

The membrane deformation energy f_s can also be viewed as a function of the average bilayer thickness change. The latter is directly related to the fractional area expansion per lipid $\Delta A/A_o$ through the chain volume conservation, where A_o is the unperturbed area per lipid and ΔA is area expansion due to the peptide adsorption. Thus the critical condition is equivalent to the condition that $\Delta A/A_o$ reaches a critical value $(\Delta A/A_o)^*$. In our previous x-ray experiment (Wu et al., 1995), DPhPC bilayer thickness changes were measured at various P/L under the condition where all of the alamethicin was adsorbed on the bilayer surface. From the bilayer thickness changes, we obtained the value $\Delta A/A_o$ for each P/L and found that ΔA is approximately $\Gamma(P/L)$, where $\Gamma \approx 280$ Å^2 is the cross section of alamethicin lying parallel to the plane of the bilayer. Thus the critical condition $(\Delta A/A_o)^*$ is equal to $\Gamma(P/L)^*/A_o$.

We now consider how this critical condition changes with the addition of PE. To do so we need to estimate the cross sections of the lipid chains and the headgroups. In our previous paper (Wu et al., 1995), the cross section of DPhPC in the L_α phase was estimated to be 76 Å^2. This was based on an estimated volume of the lipid and the smallest D spacing obtained in our x-ray experiment. The assumption was that under that condition there are three water molecules associated with each lipid molecule. This number of water molecules could have been underestimated; hence the estimate 76 Å may be the lower limit. Another way of estimating the lipid cross section is to consider the chains only. The volume of two phytanoyl chains is estimated to be 1194 Å^3 by adding the volume of 8 CH$_3$ (8 × 48.8 Å^3) to the volume of two dipalmitoyl chains (804 Å^3) (Wiener et al., 1989). Hydrated DPhPC in the L_α phase has a head-to-head distance (defined by the peaks of the electron density profile) of ~38 Å (Wu et al., 1995). From the crystal structure of dimyristoylphosphatidylcholine (Pearson and Pascher, 1979; Hauser et al., 1981), we estimate the distance from the phosphate to the midpoint between the two carbonyl groups to be ~5 Å. Thus the hydrocarbon chain thickness is ~14 Å, and the lipid cross section is ~85 Å^2. Because the phosphate-to-carbonyl distance is likely to be shorter in the L_α phase than in the crystal, 85 Å^2 is probably the upper limit. For the following numerical analysis, we use $A_o \approx 80$ Å^2 to represent the DPhPC cross section.

In the absence of peptides, the PC headgroup and its associated water must also occupy an area $A_o \approx 80$ Å^2. The experimental result $\Delta A \approx \Gamma(P/L)$ (Wu et al., 1995) suggests that, in this case, the area expansion equals the area of the added peptides. This implies that the peptide adsorption does not alter the area occupied by the PC headgroup and its associated water. We will call this the extended PC headgroup, which has a cross section $\Sigma_{PC} \approx 80$ Å^2. We assume that the size of the extended PE headgroup is proportional to

the volume of PE:

Cross section of the extended PE headgroup Σ_{PE}

$$\approx \left(\frac{\text{volume of PE}}{\text{volume of PC}}\right)\Sigma_{PC}$$

The volume of phosphorylcholine has been estimated to be 204 Å^3 (Small, 1986). From the crystal structures, the difference between the volumes of PC and PE headgroups was estimated to be 100 Å^3 (Small, 1986). Thus $\Sigma_{PE} \approx (104/204)80 \approx 40$ Å^2. When a small fraction of DPhPC ($\leq 10\%$) is replaced by DPhPE, the lipids remain in the bilayer form (at higher percentages of PE, the lipids transform to a hexagonal H$_{II}$ phase), and x-ray diffraction shows only one lamellar repeat distance, indicating that the mixtures are homogeneous (in preparation). The volume voided by the PC to PE replacement is apparently filled by water. Our assumption is that this space is available to the adsorbing peptide. This is equivalent to saying that the average size of the headgroup decreases with the percentage of PE, θ:

Average cross section of the extended head groups Σ_θ

$$= (1 - \theta)\Sigma_{PC} + \theta\Sigma_{PE}$$

We propose that the critical peptide-to-lipid ratio as a function of θ, $(P/L)^*_\theta$, satisfies the critical condition

$$\left(\frac{\Delta A}{A_o}\right)^* = \frac{\Sigma_\theta + \Gamma(P/L)^*_\theta}{A_o} - 1 \qquad (1)$$

In the absence of PE, we have $\theta = 0$, $\Sigma_o = \Sigma_{PC} = A_o \approx 80$ Å^2, and $(P/L)^*_0 \approx 1/40$. Together with $\Gamma \approx 280$ Å^2, we have $(\Delta A/A_o)^* = 7/80$. Equation 1 predicts that $(P/L)^*_{0.1} \approx 1/25$ at 10% PE and $(P/L)^*_{0.05} \approx 1/31$ at 5% PE. Both agree with the experiment (see Fig. 3) quite well.

Equation 1 can be rewritten as

$$\left(\frac{P}{L}\right)^*_\theta = \left(\frac{P}{L}\right)^*_0 + \theta\left(\frac{\Sigma_{PC} - \Sigma_{PE}}{\Gamma}\right) \qquad (2)$$

The numerical uncertainties are confined in the ratio $(\Sigma_{PC} - \Sigma_{PE})/\Gamma$. A 25% error in the estimate of this ratio will cause only a 10% error in $(P/L)^*_\theta$ when $\theta = 0.1$. So the uncertainties in the sizes of the extended headgroups are not very critical to the above comparison with experiment. The most important idea is that the critical concentration for insertion should increase with θ. This has been clearly demonstrated by our data.

The mode of action in alamethicin's role as an antibacterial peptide is the formation of pores in the membrane leading to the leakage of the cell's contents and, subsequently, cytolysis. This work provides direct evidence that the specific physical characteristics of the lipids making up the bilayer, such as the average area of the lipid headgroup versus the average lipid cross section, are important factors in determining whether alamethicin at a given concentration will perform its antibacterial function. Host-defense anti-

bacterial peptides such as magainins and cecropins discovered in frog skin (Zasloff, 1987) and in insects (Hultmark et al., 1980), respectively, function in much the same way as alamethicin, by directly attacking the cellular membrane. Each of these peptides displays a cellular specificity manifested in different threshold concentrations for lysing different varieties of cells (Jen et al., 1987; Juretic et al., 1989; Steiner et al., 1988). Magainin and cecropin are effective antibacterials at the concentrations secreted, respectively, onto the surface of the frog skin and in the insect hemolymph (Boman et al., 1994). However, their concentrations have to increase by 100–1000 times before magainin and cecropin lyse eukaryotic cells. Cellular membranes, although not as simple as a lipid bilayer, do possess specific lipid makeups for different species (Quinn and Chapman, 1980). Here we show one mechanism whereby different lipid compositions of the cellular membrane can account for some of the varying levels of effectiveness that antibacterial peptides exhibit against different types of cells.

REFERENCES

Boman, H. G., J. Marsh, and J. A. Goode, editors. 1994. Antimicrobial Peptides, Ciba Foundation Symposium 186. John Wiley and Sons, Chichester. 1–272.

Chothia, C. 1974. Hydrophobic bonding and accessible surface area in proteins. Nature. 248:338–339.

Epand, R. M., and R. Bottega. 1988. Determination of the phase behavior of phosphatidylethanolamine admixed with other lipids and the effects of calcium chloride: implications for protein kinase C regulation. Biochim. Biophys. Acta. 944:144–154.

Gruner, S. M. 1994. Couping between bilayer curvature elasticity and membrane protein activity. In Biomembrane Electrochemistry. M. Blank and I. Vodyanoy, editors. American Chemical Society, Washington, DC. 129–149.

Hah, J. S., S. W. Hui, and C. Y. Jung. 1993. Effects of physical states of phospholipids on the incorporation and cytochalasin B binding activity of human erythrocyte membrane proteins in reconstituted vesicles. Biochemistry. 22:4763–4769.

Hauser, H., I. Pascher, R. H. Pearson, and S. Sundell. 1981. Preferred conformation and molecular packing of phosphatidylethanolamine and phosphatidylcholine. Biochim. Biophys. Acta. 650:21–51.

He, K., S. J. Ludtke, W. T. Heller, and H. W. Huang. 1996a. Mechanism of alamethicin insertion into lipid bilayers. Biophys. J. 71:2669–2679.

He, K., S. J. Ludtke, D. I. Worcester, and H. W. Huang. 1995. Antimicrobial peptide pores in membranes detected by neutron in-plane scattering. Biochemistry. 34:15614–15618.

He, K., S. J. Ludtke, D. I. Worcester, and H. W. Huang. 1996b. Neutron scattering in the plane of membrane: structure of alamethicin pores. Biophys. J. 70:2659–2666.

Huang, H. W. 1995. Elasticity of lipid bilayer interaction with amphipilic helical peptides. J. Phys. II France. 5:1427–1431.

Huang, H. W., and G. A. Olah. 1987. Uniformly oriented gramicidin channels embedded in thick monodomain lecithin multilayers. Biophys. J. 51:989–992.

Huang, H. W., and Y. Wu. 1991. Lipid-alamethicin interactions influence alamethicin orientation. Biophys. J. 60:1079–1087.

Hui, S. W., T. P. Stewart, P. L. Yeagle, and A. D. Albert. 1981. Bilayer to non-bilayer transition in mixtures of of phosphatidylethanolamine and phosphatidylcholine: implications for membrane properties. Arch. Biochem. Biophys. 207:227–240.

Hultmark, D., H. Steiner, T. Rasmuson, and H. G. Bowman. 1980. Insect immunity: purification and properties of three inducible bactericidal proteins from hemolymph of immunized pupae of Hyalophora cecropia. Eur. J. Biochem. 106:7–16.

Jen, W.-C., G. A. Jones, D. Brewer, V. O. Parkinson, and A. Taylor. 1987. The antibacterial activity of alamethicin and zervamicins. J. Appl. Bacteriol. 63:293–298.

Juretic, D., H.-C. Chen, J. H. Brown, J. L. Morell, R. W. Hendler, and H. V. Westerhoff. 1989. Magainin 2 amide and analogues. FEBS Lett. 249:219–223.

Keller, S. L., S. M. Bezrukov, S. M. Gruner, M. W. Tate, I. Vodyanoy, and V. A. Parsegian. 1993. Probability of alamethicin conductance states varies with nonlamellar tendency of bilayer phospholipids. Biophys. J. 65:23–27.

Kirk, G. L., and S. M. Gruner. 1985. Lyotropic effects of alkanes and headgroup composition on the L_α-H_{II} lipid liquid crystal phase transition: hydrocarbon packing versus intrinsic curvature. J. Physique. 46:761–769.

Ludtke, S. J., K. He, W. T. Heller, T. A. Harroun, L. Yang, and H. W. Huang. 1996. Membrane pores induced by magainin. Biophys. J. 35: 13723–13728.

Ludtke, S. J., K. He, and H. W. Huang. 1995. Membrane thinning caused by magainin 2. Biochemistry. 34:16764–16769.

Merrifield, R. B., E. L. Merrifield, P. Juvvadi, D. Andreu, and H. G. Boman. 1994. Design and synthesis of antimicrobial peptides. In Antimicrobial Peptides, Ciba Foundation Symposium 186. H. G. Boman, J. Marsh, and J. A. Goode, editors. John Wiley and Sons, Chichester. 5–26.

Nagle, J. F., and D. A. Wilkinson. 1978. Lecithin bilayers: density measurements and molecular interactions. Biophys. J. 23:159–175.

Pandey, R. C., J. C. Cook, and K. L. Rinehart. 1977. High resolution and field desorption mass spectrometry studies and revised structure of alamethicin I and II. J. Am. Chem. Soc. 99:8469–8483.

Pearson, R. H., and I. Pascher. 1979. The molecular structure of lecithin dihydrate. Nature. 281:499–501.

Quinn, P. J. and D. Chapman. 1980. The dynamics of membrane structure. CRC Crit. Rev. Biochem. 8:1–117.

Small, D. M. 1986. The Physical Chemistry of Lipids. Plenum Press, New York. 479–512.

Steiner, H., D. Andreu, and R. B. Merrifield. 1988. Binding and action of cecropin and cecropin analogues: antibacterial peptides from insects. Biochim. Biophys. Acta. 939:260–266.

Wiener, M. C., R. M. Suter, and J. F. Nagle. 1989. Structure of the fully hydrated gel phase of dipalmitoylphosphatidylcholine. Biophys. J. 55: 315–325.

Wu, Y., K. He, S. J. Ludtke, and H. W. Huang. 1995. X-ray diffraction study of lipid bilayer membrane interacting with amphiphilic helical peptides: diphytanoyl phosphatidylcholine with alamethicin at low concentrations. Biophys. J. 68:2361–2369.

Wu, Y., H. W. Huang, and G. A. Olah. 1990. Method of oriented circular dichroism. Biophys. J. 57:797–806.

Zasloff, M. 1987. Magainins, a class of antimicrobial peptides form Xenopus skin: isolation, characterization of two active forms and partial cDNA sequence of a precursor. Proc. Natl. Acad. Sci. USA. 84: 5449–5453.